

# Anharmonicity-Driven low Lattice Thermal Conductivity and High Thermoelectric Response in Monolayer $\text{CeX}_2$ ( $\text{X}=\text{O}, \text{S}, \text{Se},$ $\text{Te}$ )

Ziyi Pan,<sup>1</sup> Daxue Hao,<sup>1</sup> Wenjie Xiong,<sup>1</sup> Geng Li,<sup>2,3,\*</sup> Jinpeng Yang,<sup>1,†</sup> and Shuming Zeng<sup>1,‡</sup>

<sup>1</sup>*College of Physics Science and Technology,  
Yangzhou University, Jiangsu 225009, China*

<sup>2</sup>*China Rare Earth Group Research Institute,  
Shenzhen, Guangdong, 518000, China*

<sup>3</sup>*Key Laboratory of Rare Earths, Ganjiang Innovation Academy,  
Chinese Academy of Sciences, Ganzhou, 341000, China*

(Dated: January 15, 2026)

---

\* geng'li@regcc.cn

† yangjp@yzu.edu.cn

‡ zengsm@yzu.edu.cn

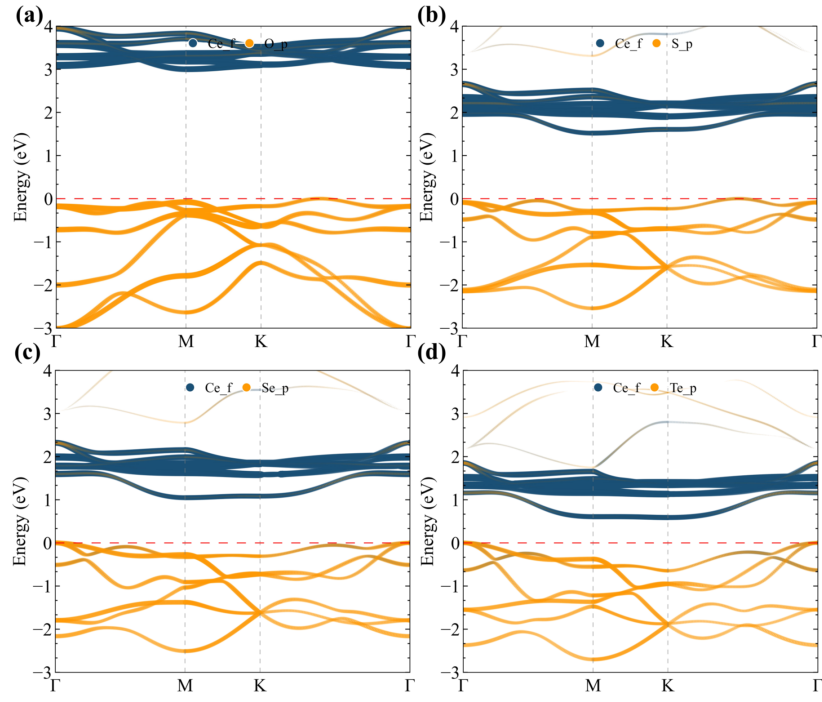


FIG. S1. Orbital-projected band structures of  $\text{CeX}_2$ .

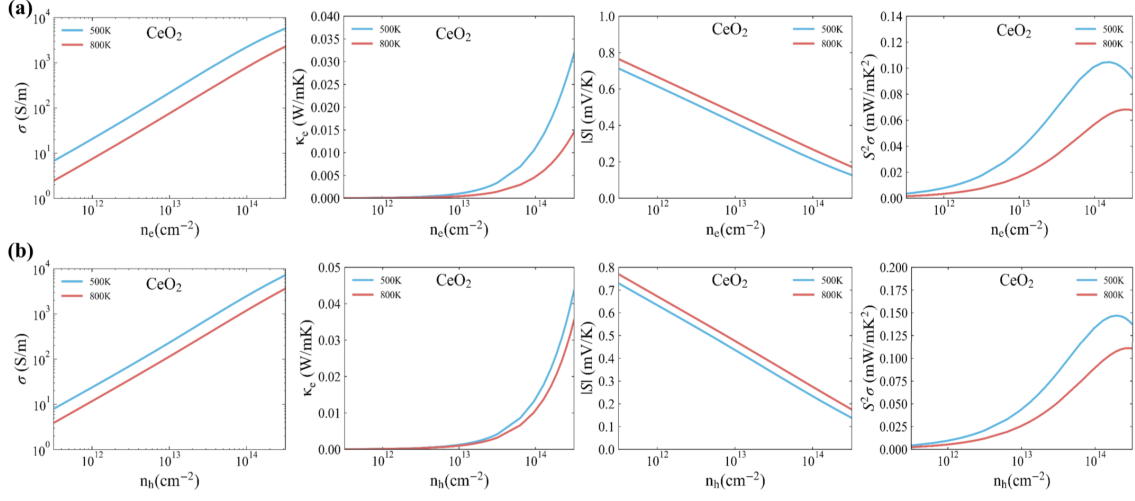


FIG. S2. The calculated electrical conductivity ( $\sigma$ ), Seebeck coefficient ( $S$ ), electronic thermal conductivity ( $\kappa_e$ ) and power factor ( $PF = S^2\sigma$ ) at 500 and 800 K without SOC for (a) n-type and (b) p-type  $\text{CeO}_2$ .

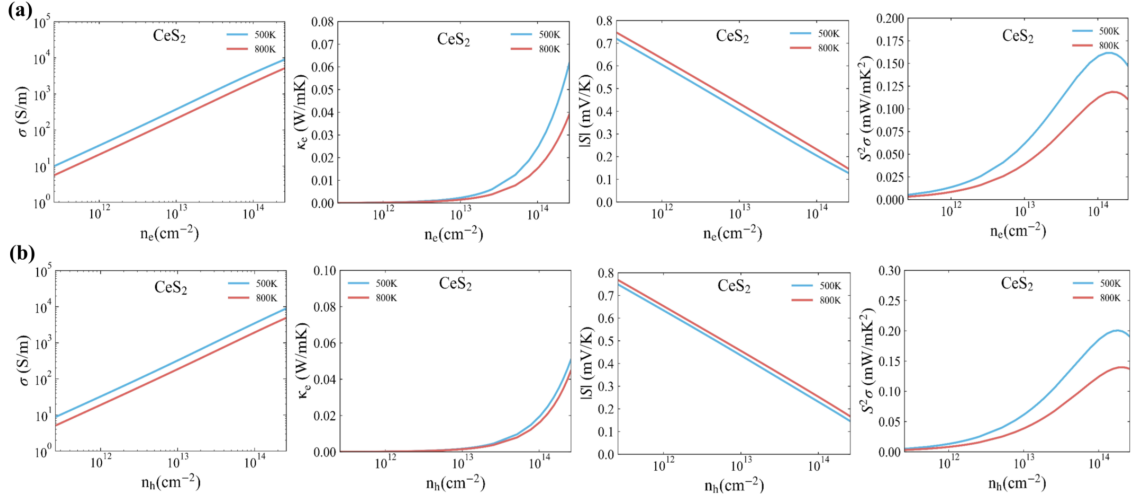


FIG. S3. The calculated electrical conductivity ( $\sigma$ ), Seebeck coefficient ( $S$ ), electronic thermal conductivity ( $\kappa_e$ ) and power factor ( $PF = S^2\sigma$ ) at 500 and 800 K without SOC for (a) n-type and (b) p-type  $\text{CeS}_2$ .

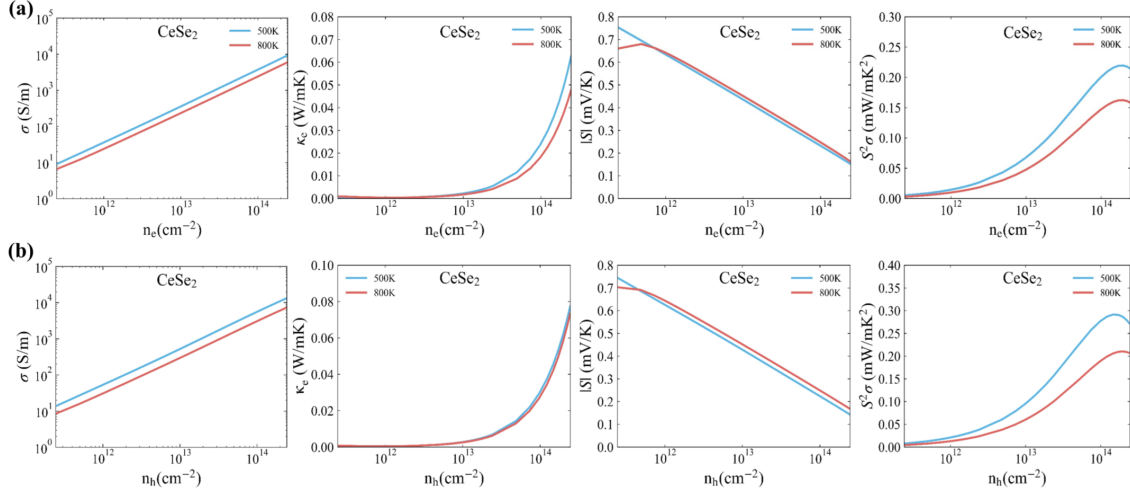


FIG. S4. The calculated electrical conductivity ( $\sigma$ ), Seebeck coefficient ( $S$ ), electronic thermal conductivity ( $\kappa_e$ ) and power factor ( $PF = S^2\sigma$ ) at 500 and 800 K without SOC for (a) n-type and (b) p-type CeSe<sub>2</sub>.

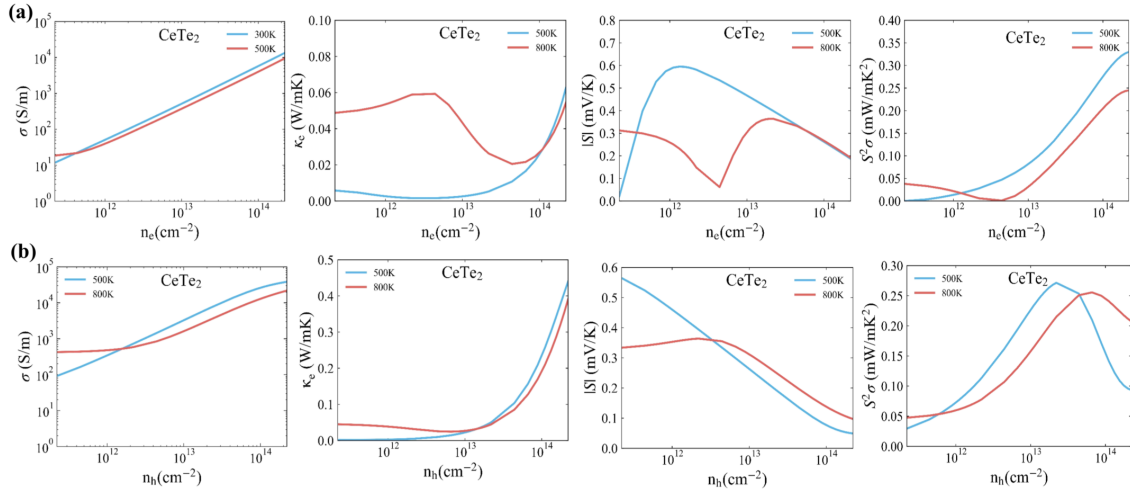


FIG. S5. The calculated electrical conductivity ( $\sigma$ ), Seebeck coefficient ( $S$ ), electronic thermal conductivity ( $\kappa_e$ ) and power factor ( $PF = S^2\sigma$ ) at 500 and 800 K without SOC for (a) n-type and (b) p-type CeTe<sub>2</sub>.

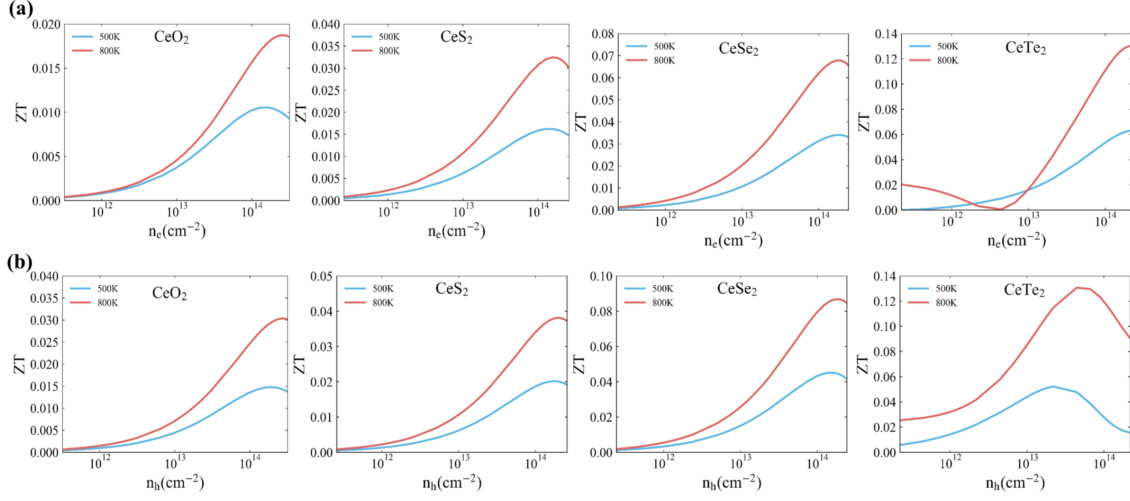


FIG. S6. The calculated  $ZT$  at 500 and 800 K without SOC for (a) n-type and (b) p-type  $CeX_2$ .

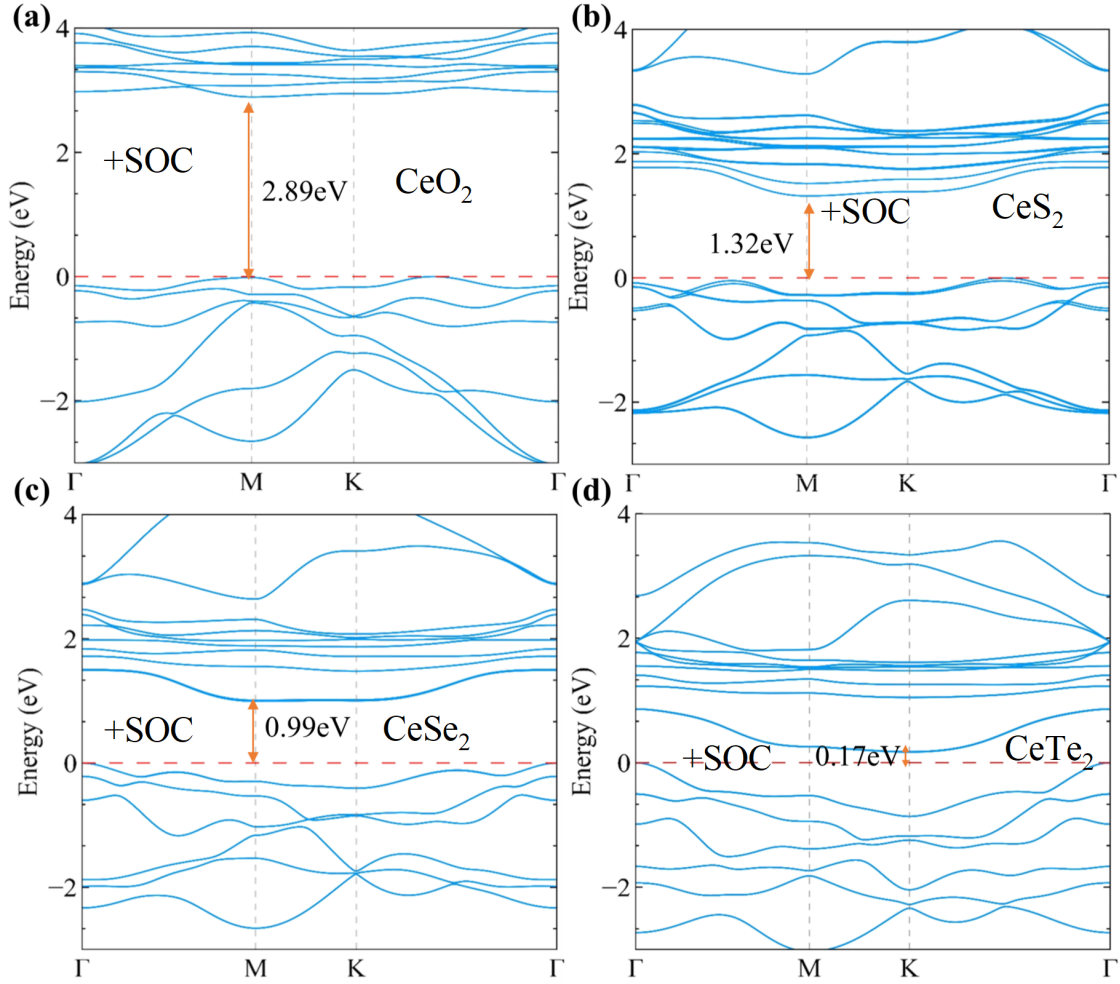


FIG. S7. The calculated band structures with SOC for (a)  $CeO_2$ , (b)  $CeS_2$ , (c)  $CeSe_2$  and (d)  $CeTe_2$ .

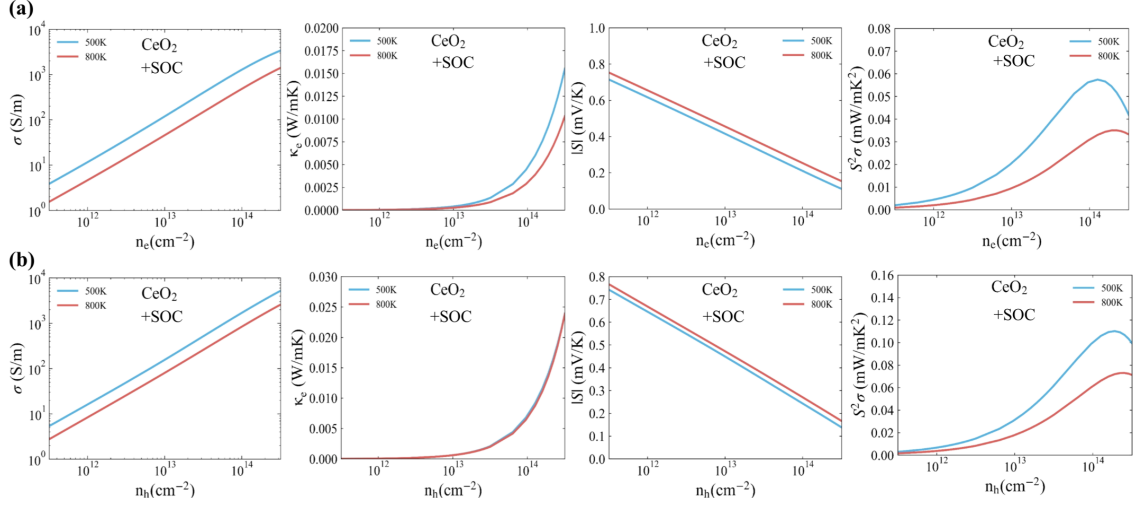


FIG. S8. The calculated electrical conductivity ( $\sigma$ ), Seebeck coefficient ( $S$ ), electronic thermal conductivity ( $\kappa_e$ ) and power factor ( $PF = S^2\sigma$ ) at 500 and 800 K with SOC for (a) n-type and (b) p-type  $\text{CeO}_2$ .

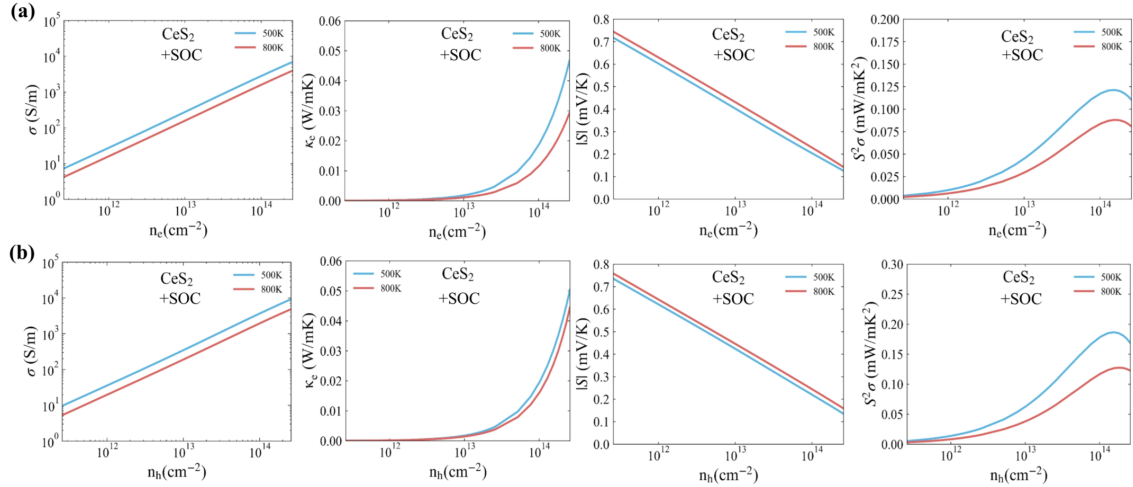


FIG. S9. The calculated electrical conductivity ( $\sigma$ ), Seebeck coefficient ( $S$ ), electronic thermal conductivity ( $\kappa_e$ ) and power factor ( $PF = S^2\sigma$ ) at 500 and 800 K with SOC for (a) n-type and (b) p-type  $\text{CeS}_2$ .

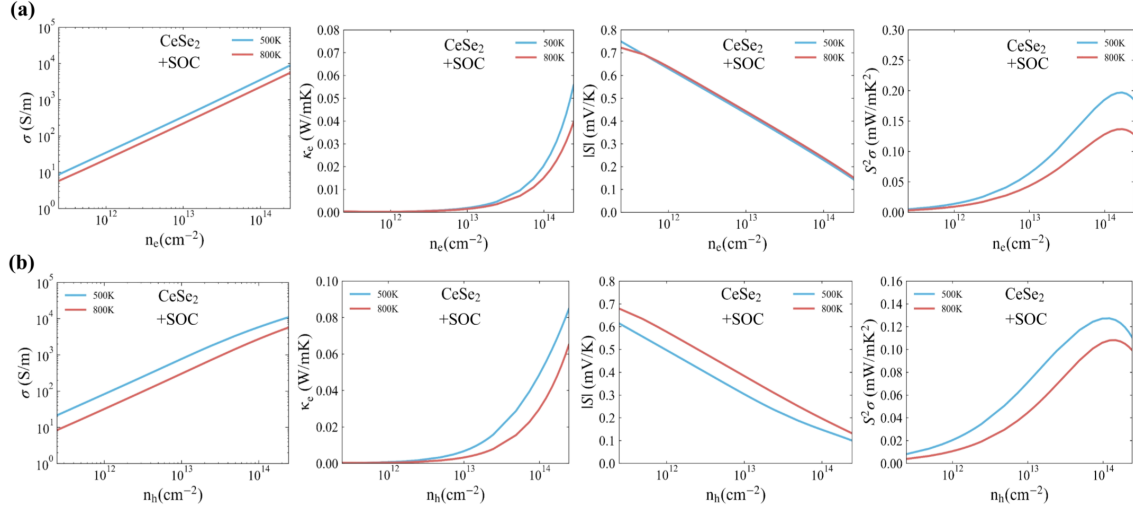


FIG. S10. The calculated electrical conductivity ( $\sigma$ ), Seebeck coefficient ( $S$ ), electronic thermal conductivity ( $\kappa_e$ ) and power factor ( $\text{PF} = S^2\sigma$ ) at 500 and 800 K with SOC for (a) n-type and (b) p-type  $\text{CeSe}_2$ .

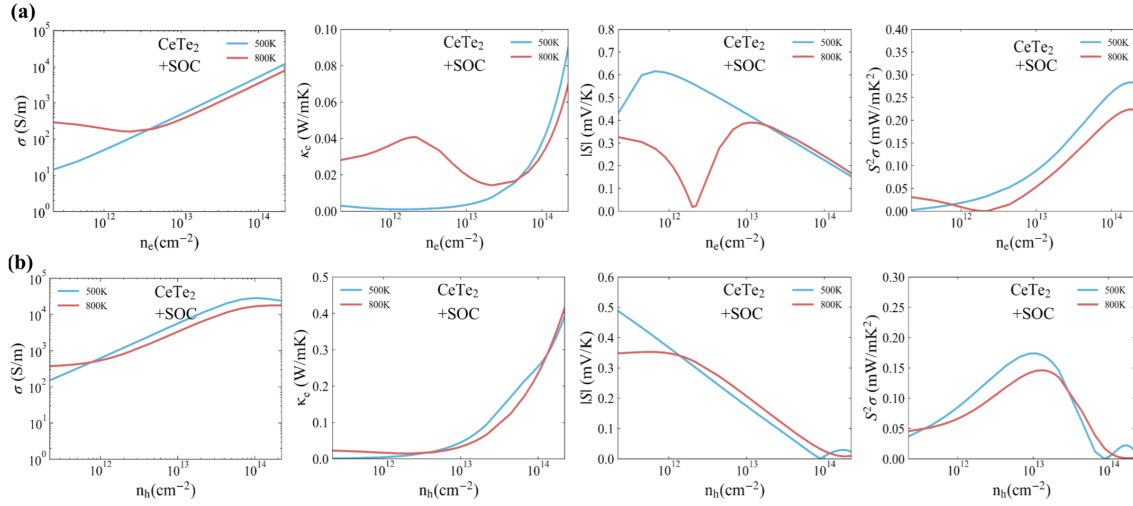


FIG. S11. The calculated electrical conductivity ( $\sigma$ ), Seebeck coefficient ( $S$ ), electronic thermal conductivity ( $\kappa_e$ ) and power factor ( $\text{PF} = S^2\sigma$ ) at 500 and 800 K with SOC for (a) n-type and (b) p-type  $\text{CeTe}_2$ .

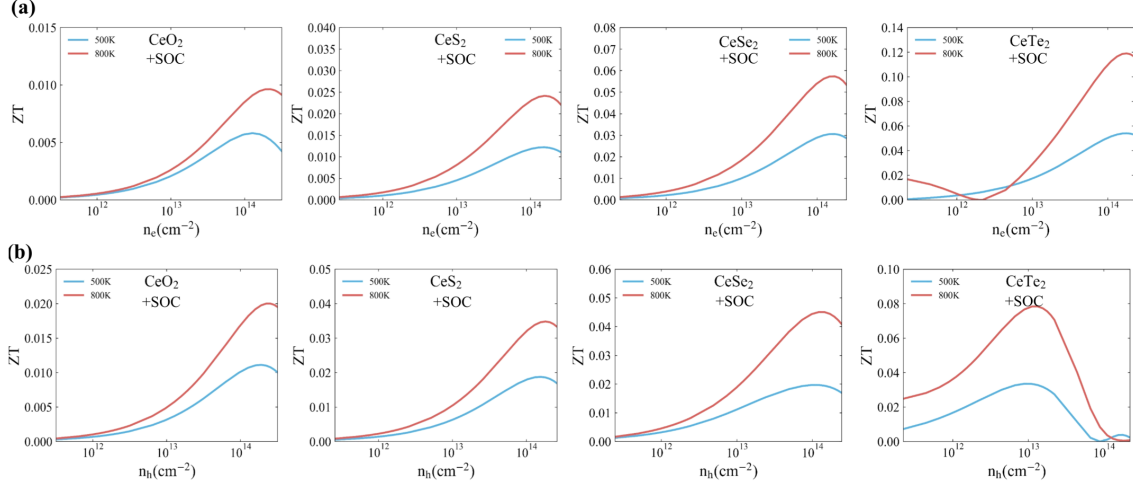


FIG. S12. The calculated  $ZT$  at 500 and 800 K with SOC for (a) n-type and (b) p-type  $CeX_2$ .

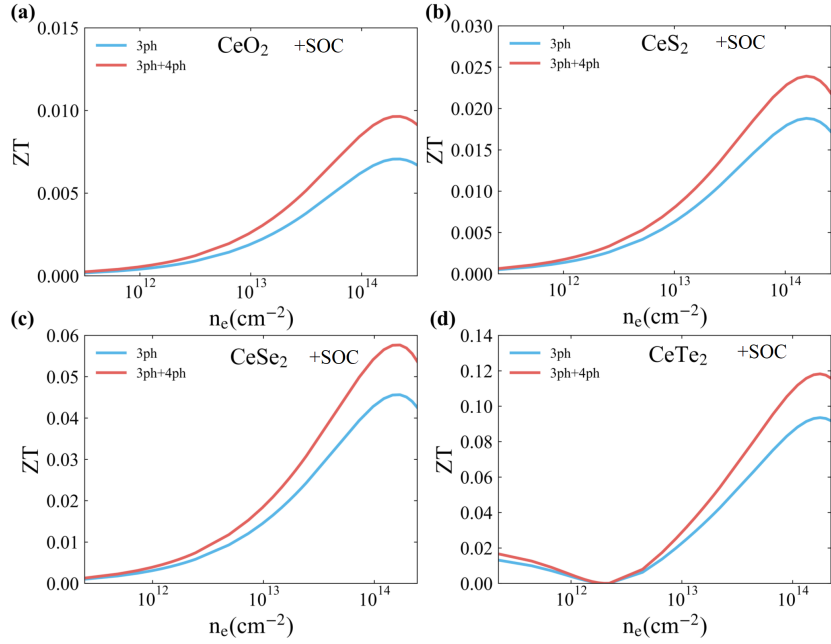


FIG. S13. The calculated  $ZT$  at 800 K for n-type (a)  $CeO_2$ , (b)  $CeS_2$ , (c)  $CeSe_2$  and (d)  $CeTe_2$  with and without 4ph scattering.

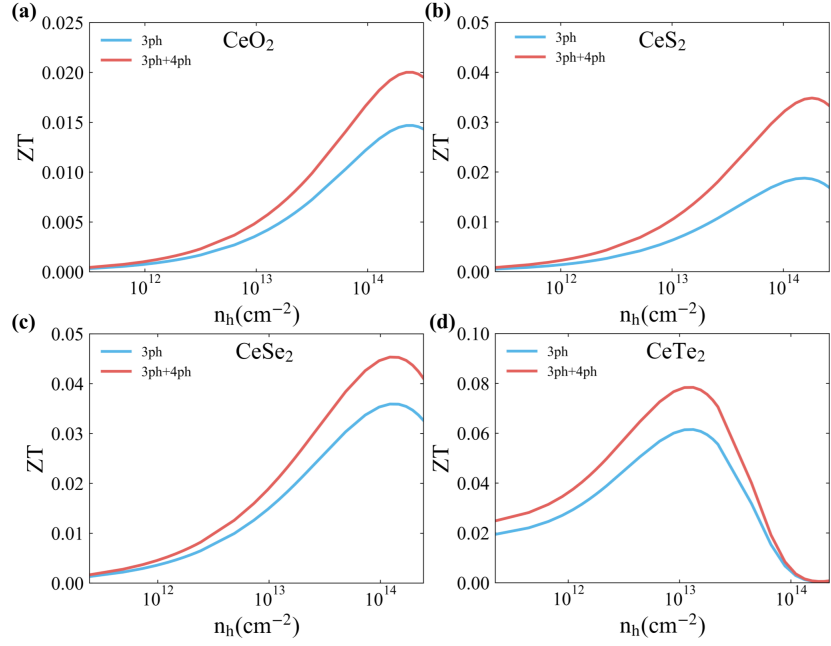


FIG. S14. The calculated  $ZT$  at 800 K for p-type (a)  $\text{CeO}_2$ , (b)  $\text{CeS}_2$ , (c)  $\text{CeSe}_2$  and (d)  $\text{CeTe}_2$  with and without 4ph scattering.